



Since January 2020 Elsevier has created a COVID-19 resource centre with free information in English and Mandarin on the novel coronavirus COVID-19. The COVID-19 resource centre is hosted on Elsevier Connect, the company's public news and information website.

Elsevier hereby grants permission to make all its COVID-19-related research that is available on the COVID-19 resource centre - including this research content - immediately available in PubMed Central and other publicly funded repositories, such as the WHO COVID database with rights for unrestricted research re-use and analyses in any form or by any means with acknowledgement of the original source. These permissions are granted for free by Elsevier for as long as the COVID-19 resource centre remains active.



# Comparative evaluation of integrated purification pathways for bacterial modular polyomavirus major capsid protein VP1 to produce virus-like particles using high throughput process technologies

Lukas Gerstweiler<sup>a</sup>, Jagan Billakanti<sup>b</sup>, Jingxiu Bi<sup>a</sup>, Anton Middelberg<sup>c,\*</sup>

<sup>a</sup> The University of Adelaide, School of Chemical Engineering and Advanced Materials, Adelaide, SA 5005, Australia

<sup>b</sup> Cytiva, Product and Application Specialist Downstream Design-In ANZ, Suite 547, Level 5, 7 Eden Park Drive, Macquarie Park, NSW 2113, Australia

<sup>c</sup> The University of Adelaide, Division of Research and Innovation, Adelaide, SA 5005, Australia

## ARTICLE INFO

### Article history:

Received 10 November 2020

Revised 11 January 2021

Accepted 16 January 2021

Available online 21 January 2021

### Keywords:

Virus-like particles

Downstream processing

VP1

High-throughput development

Multi modal chromatography

## ABSTRACT

Modular virus-like particles and capsomeres are potential vaccine candidates that can induce strong immune responses. There are many described protocols for the purification of microbially-produced viral protein in the literature, however, they suffer from inherent limitations in efficiency, scalability and overall process costs. In this study, we investigated alternative purification pathways to identify and optimise a suitable purification pathway to overcome some of the current challenges. Among the methods, the optimised purification strategy consists of an anion exchange step in flow through mode followed by a multi modal cation exchange step in bind and elute mode. This approach allows an integrated process without any buffer adjustment between the purification steps. The major contaminants like host cell proteins, DNA and aggregates can be efficiently removed by the optimised strategy, without the need for a size exclusion polishing chromatography step, which otherwise could complicate the process scalability and increase overall cost. High throughput process technology studies were conducted to optimise binding and elution conditions for multi modal cation exchanger, Capto<sup>TM</sup> MMC and strong anion exchanger Capto<sup>TM</sup> Q. A dynamic binding capacity of 14 mg ml<sup>-1</sup> was achieved for Capto<sup>TM</sup> MMC resin. Samples derived from each purification process were thoroughly characterized by RP-HPLC, SEC-HPLC, SDS-PAGE and LC-ESI-MS/MS Mass Spectrometry analytical methods. Modular polyomavirus major capsid protein could be purified within hours using the optimised process achieving purities above 87% and above 96% with inclusion of an initial precipitation step. Purified capsid protein could be easily assembled *in-vitro* into well-defined virus-like particles by lowering pH with addition of calcium chloride to the eluate. High throughput studies allowed the screening of a vast design space within weeks, rather than months, and unveiled complicated binding behaviour for Capto<sup>TM</sup> MMC.

© 2021 Elsevier B.V. All rights reserved.

## 1. Introduction

The current outbreak of COVID-19 shows dramatically the threat of global pandemics and the need for potent vaccines that can be mass-manufactured efficiently. In a globally-mobile world pathogens such as corona virus, influenza virus, Ebola virus etc. can spread rapidly so keeping a local outbreak under control is challenging. Once emerged a sustainable control can only be achieved by mass vaccination as demonstrated for example for Polio and Measles [1–3]. An ideal vaccine candidate to do so is highly immunogenic, exceptionally safe and can be quickly mass produced. Another important point that is often neglected is the

need for low production costs, thus enabling affordable to use in low income countries, which often suffer the most from infectious diseases and otherwise may function as a residual reservoir for global threat [4,5]. Conventional vaccines such as inactivated and attenuated viruses however, have a lengthy production time, expensive production costs and might be risky for people with immunodeficiency [6,7].

Promising future vaccine candidates that incorporate most of the desired properties are virus-like particles (VLPs). VLPs are self-assembled spherical particles of viral structural proteins, mimicking the overall appearance and structure of a native virus and due to a lack of genetic material are unable to replicate or infect, making them generally safe [8]. As the antigens are presented in a highly repetitive and native structure, VLPs induce a strong immunogenic response both humoral and cellular, even

\* Corresponding author.

E-mail address: [anton.middelberg@adelaide.edu.au](mailto:anton.middelberg@adelaide.edu.au) (A. Middelberg).

in the absence of any adjuvant [9]. The structural viral proteins can be amended to present foreign antigens on the surface of the VLP. These so called modular or chimeric VLPs widen the possible applications and enabled the development of vaccine platform technologies [10,11]. VLPs as vaccines are commercially available against human papilloma virus and hepatitis B/E virus (Cervarix®, Gardasil®, Cecolin®, Recombivax HB®, Energix-B®, Hecolin® etc.) and are heavily examined against many diverse pathogens including influenza A, Norovirus, Chikungunya virus, cytomegalovirus, rotavirus and Group A Streptococcus, to name a few [8,12–15]. However, the production and purification of existing commercial VLPs is challenging, making them comparatively expensive vaccines [11,16,17]. VLPs can be expressed in a variety of eukaryotic and prokaryotic systems, ranging from mammalian and insect cells to microbial, yeast and plant based systems [18]. Expression in eukaryotic cells leads to self-assembly of VLPs *in vivo*, which always bears the risk of co-assembled impurities such as host cell proteins and nucleic acids, therefore leading to product deviations that require a subsequent disassembly-reassembly step [19,20]. Another pathway is the expression in prokaryotic systems, which allow the purification of unassembled structural protein and a subsequent *in vitro* assembly in a controlled environment [20–22].

VLPs produced in a prokaryotic expression system are an exciting alternative due to their inherent advantages over eukaryotic ones in terms of speed and productivity, enabling possible costs of cents per vaccine dose [23–25]. China approved *E. coli* produced VLP vaccines Hecolin® and Cecolin® showing high efficiency and safety and providing proof of concept for *E. coli* produced VLP vaccines [26,27]. Several modular and non-modular VLPs based on a variety of structural viral protein such as hepatitis B core antigen (HBcAg), papilloma major capsid protein L1, bacteriophage Q $\beta$ , adeno-associated virus structural protein VP3 and polyomavirus major capsid protein VP1 have been produced in *E. coli* [24,25,28,29]. One of the most advanced approaches is the platform technology using modularized murine polyomavirus major capsid protein VP1 [10]. The viral protein can be expressed at grams per litre in *E. coli* giving VLPs able to induce a strong immune response against Group A Streptococcus, Influenza, Rotavirus, Plasmodium, and others [12,13,30–33]. However, described purification and production pathways for VP1, the related L1 and other microbial VLPs currently rely on hard-to-scale laboratory unit operations. Major issues during purification are the removal of DNA and aggregates and low binding on chromatographic resin caused by aggregates and the large size of capsomeres and VLPs [34–37]. Common practice is the use of affinity tags (GST, poly HIS, SUMO), which require a subsequent enzymatic cleavage and removal of the tag, leading to aggregation during long processing times and other process challenges, and subsequent preparative size exclusion chromatography (SEC) followed by dialysis to trigger assembly [10,34,38,39]. Other described pathways use furthermore various combinations of density gradient centrifugation, benzonase treatment, filtration, membrane columns, refolding of inclusion bodies and ammonium sulphate/PEG precipitation [27,34,35,40–42].

To overcome these challenges, we developed and optimised an integrated purification process using multi modal cation exchanger Capto™ MMC as the main purification step. Multi modal ion exchange resin combines ion exchange with hydrophobic interaction and other modes, which lead to unique binding behaviour and high salt tolerance [43]. The salt tolerance of Capto™ MMC enables processing at intermediate salt concentrations, which enables disaggregation of non-specific DNA-protein interactions, which otherwise hinder separation. The developed process produces well defined VLPs, removes aggregates, DNA and most host cell proteins, is designed for scale-up and does not require any buffer exchange during the optimized purification process, thus reducing overall process cost and time.

## 2. Material and methods

### 2.1. Buffers and chemicals

Milli-Q® water (MQW) was used for the preparation of all buffers. *E. coli* culture was grown in Terrific Broth (TB) medium (12 g l<sup>-1</sup> tryptone (LP0042, Thermo Fisher Scientific, USA), 24 g l<sup>-1</sup> yeast extract (P0021, Thermo Fisher Scientific, USA), 5 g l<sup>-1</sup> Glycerol (GL010, ChemSupply, Australia), 2.31 g l<sup>-1</sup> potassium dihydrogen phosphate (PO02600, ChemSupply Australia), 12.5 g l<sup>-1</sup> dipotassium hydrogen phosphate (PA020, ChemSupply, Australia)), supplemented with 35  $\mu$ g ml<sup>-1</sup> chloramphenicol (GA0258, ChemSupply, Australia) and 100  $\mu$ g ml<sup>-1</sup> ampicillin (GA0283, ChemSupply, Australia). IPTG (15529019, Thermo Fisher Scientific, USA) and antibiotics were prepared in 1000x stock solutions and added before use. Sodium chloride (SL046, ChemSupply, Australia) solution, 9 g l<sup>-1</sup>, was used as a washing saline.

Loading buffer (L buffer) consisted of 40mM buffer salt (Tris-hydrochloride (GB4431, ChemSupply, Australia) for pH 8 and 9, Glycine (GA007, ChemSupply, Australia) for pH 10 and sodium hydrogen orthophosphate (SL061, ChemSupply, Australia) for pH 11 and 12 buffer preparation) plus 2mM EDTA (EA023, ChemSupply, Australia), 5 % w w<sup>-1</sup> glycerol, 5mM dithiothreitol (DTT) (DL131, ChemSupply, Australia) and 0–500 mM NaCl (SL046, ChemSupply, Australia). DTT and 1x SigmaFast™ protease inhibitor (SA8820 Millipore Sigma, USA), which were added during cell lysis, were added freshly before use. Loading buffer was prepared from a 5x stock solution originally prepared, filtered (0.2  $\mu$ m, KYL Scientific, Australia) and vacuum degassed before use. Calcium chloride (CA033, ChemSupply, Australia) was used to induce the assembly of VLPs.

TruPAGE™ 4x LDS sample buffer (PCG3009) and 20x Tris-MOPS SDS express running buffer (PCG3003) were purchased from MilliporeSigma, USA. The 10x DTT sample reducer and 800x running oxidant (sodium bisulfite, 243973, Millipore Sigma, USA) reagents were freshly prepared before use. For staining of SDS-APGE gels a solution containing Coomassie Brilliant Blue R-250 (Bio-Rad Laboratories, USA), and for destaining a mixture of 10 % v v<sup>-1</sup> ethanol (EA043, ChemSupply, Australia) and 10 % v v<sup>-1</sup> acetic acid (AA009, ChemSupply, Australia) was used.

HPLC grade acetonitrile (LC1005) and Trifluoroacetic Acid (TFA) (TS181) were purchased from Chem-Supply, Australia

PEG-6000 (PL113, ChemSupply, Australia) was used for precipitation experiments.

### 2.2. Plasmid construction and protein expression

Group A Streptococcus antigen GCN4-J8 was inserted with flanking G4S linkers into murine polyomavirus major capsid protein VP1 sequence (M34958) and cloned into pETDuet-1 at multiple cloning site 2 (MCS2) at *Nde*I and *Pac*I restriction sites. The plasmid was constructed by the Protein Expression Facility of the University of Queensland, Brisbane, Australia and the sequence was verified by the Australian Genome Research facility (AGRF), Brisbane, Australia.

Rosetta™ 2(DE3) Singles™ competent cells (Merck KGaA, Germany) were used as an expression system. The VP1-J8 plasmid was transformed by heat shock transformation. In brief, competent cells were mixed with plasmid DNA and incubated on ice for 5 min, followed by a heat shock at 42°C for 30 s and 2 min cooling on ice. Subsequently, they were diluted with TOC medium and inoculated on TB agar plates containing 100  $\mu$ g ml<sup>-1</sup> ampicillin and 35  $\mu$ g ml<sup>-1</sup> chloramphenicol. The Master Cell Bank (MCB) glycerol stocks were produced by growing a single colony at 37°C in 50 ml TB medium in a 250 ml shake flask until an optical density OD<sub>600</sub> of 0.5 AU was reached and subsequent adding of glycerol to a fi-

nal concentration of 25 % w w<sup>-1</sup>. Samples of 100 µl were collected and vials stored at -80°C until further use.

Cells were grown overnight in 50 ml of TB medium containing 35 µg ml<sup>-1</sup> chloramphenicol and 100 µg ml<sup>-1</sup> ampicillin in a 250 ml shake flask at 37°C and 200 rpm. A 5 ml sample of the overnight culture was transferred into a 200 ml of fresh TB medium in a 1 l shake flask and cells were grown under the same conditions till an OD<sub>600</sub> of 0.5 AU was reached. Protein expression was induced by adding IPTG to a final concentration of 0.1 mmol and performed for 16 h at a reduced temperature of 27°C and 200 rpm. Cells were harvested by centrifugation in an A5920R centrifuge (Eppendorf, Germany) at 3200 g for 10 min at 4°C, resuspended in 0.9 % w w<sup>-1</sup> saline and split into 50 ml aliquots. After centrifugation for 10 min at 20,130 g at 4°C the supernatant was discarded and the pellets were stored at -80°C until further process.

Clarified lysate was produced by resuspending approximately 1 g of cell pellet per 50 ml of L buffer pH 8, 0 M NaCl on ice. Cells were disrupted by ultrasonic homogenization using a Scientz-UIID Ultrasonic homogeniser (Ningbo Scientz Biotechnology, China) equipped with a 6 mm diameter horn. The suspension was sonicated with 10 s bursts at 400 W followed by 40 s cool down on ice, for a total time of 15 min. Subsequently the lysed cell suspension was centrifuged for 45 min at 20130 g at 4°C to remove cell debris.

### 2.3. Characterisation

Expression was visualised by SDS-PAGE analysis under reducing and denaturing conditions using TruPAGE™ precast Gels 4-12 %, 10 × 10 cm 12-well (PCG2003, Millipore Sigma, USA), following the manufacturer's protocol. Total protein concentration of the samples was measured by Bradford protein assay and the amount of protein loaded on each well was normalised. Samples were prepared by mixing with 4X loading buffer prior heating for 10 min at 75°C. Gel electrophoresis carried out at 180 V fixed current was applied for separation until finished, followed by 1 h of staining and 4 h of destaining using the described buffers. Precision Plus Protein™ Standard (1610363, Bio-Rad, USA) was used as a protein marker.

Bradford Protein Assay for determination of total protein concentration used standard protocol as described by BioRad in 200 µl 96 well plates format [44]. As a reference bovine serum albumin was used. Concentration of the reference solutions was verified by A<sub>280</sub> absorbance on a NanoDrop™ (Thermo Fisher Scientific, USA).

Quant-iT™ High-Sensitivity dsDNA Assay Kit (Q33232, Thermo Fisher Scientific, USA) was used for quantification of host cell DNA. Fluorescence at 485/530 nm was measured on a 2300 Victor X5 multilabel reader (PerkinElmer, US). The DNA content is given as g<sub>DNA</sub> g<sub>protein</sub><sup>-1</sup>, which is measured by Bradford.

VP1-J8 concentration was measured by RP-HPLC using a method described in the literature [45–47], on a Shimadzu UFLC-XR system (pump: LC-20AD-XR, autosampler: SIL-20AXR, diode array detector: SPD-M20A, column oven: CTO-20) with detection at 280 nm. A Vydac Protein C4 column 2.1 × 100 mm, 5 µm (214TP521) was used. Briefly, samples were mixed 1:4 with denaturing buffer (8 M guanidine (GE1914, ChemSupply, Australia), 50 mM DTT, 20 mM Tris pH 8) and incubated at 75°C for 10 min. Samples, 3 µl, were injected and separated by gradient elution with a water (Mobile Phase A, 0.5 % TFA) and acetonitrile (Mobile Phase B, 0.4 % TFA) system. The elution program was as following: 6 min gradient from 35 % B to 60 % B, 30 s gradient from 60 % B to 100 % B, 1 min 100 % B, 30 s from 100 % B to 35 % B and 4 min of 35 % B, giving a total analysis time of 12 min, at a flow rate of 1 ml min<sup>-1</sup> and a column temperature of 60°C. As a reference purified VP1-J8 was used of which the concentration was determined by Bradford assay.

The same Shimadzu system was used for SEC-HPLC with a TSKgel G3000SW column (5 µm, 7.8 × 300 mm, Tosoh Corp.). 40 % v v<sup>-1</sup> acetonitrile, 0.1 v v<sup>-1</sup> TFA was used as a running buffer at a flow rate of 1 ml min<sup>-1</sup> and 30°C column temperature. Samples received no pre-treatment except filtering through a 0.22 µm cellulose acetate filter (THCCH2213, Thermo Fisher Scientific, USA). The peak areas at A<sub>280</sub> nm were analysed and categorized into high-molecular-weight impurities (HMWI) and low-molecular-weight (LMHI) impurities depending on if they elute before or after the VP1-J8 peak. An example chromatogram can be found in the appendix (figure A1).

Aggregates were quantified by SEC chromatography with a Superose® 6 Increase 10/300 GL (Cytiva, Sweden) with L buffer pH 8, 0.5 M NaCl as a running buffer and a flow rate of 0.6 ml min<sup>-1</sup> on an ÄKTA pure system equipped with a sample pump (Cytiva, Sweden). Aggregates have been defined as the fraction remaining in the excluded volume of the Superose® 6 column. The identity as VP1-J8 aggregates was verified by SDS-PAGE. Absorbance was measured at 280 nm and 260 nm. Aggregates are expressed as the peak area in relation to the VP1-J8 peak area.

Liquid chromatography–electrospray ionisation tandem mass spectrometry (LC-ESI-MS/MS) was used to analyse and identify the protein bands in the purified samples. Mass spectrometric analysis was performed at the Adelaide Proteomic Centre, University of Adelaide. In brief gel bands were destained and dried followed by in-gel reduction plus alkylation and subsequent trypsin digestion. Peptide separation was performed using a 75 µm ID C18 column (Acclaim PepMap100 C18 75 µm × 15 cm, Thermo-Fisher Scientific, USA). Raw MS/MS data was searched against the target sequence of VP1-J8 and *E. coli* entries present in the Swiss-Prot database in Proteome Discovery (v.2.4, Thermo-Fisher Scientific, USA). Full protocol can be found in appendix.

Transmission electron microscopy (TEM) was used to analyse VLPs. Samples of 5 µl were diluted 1:10 with MQW and pipetted on carbon coated square meshed grids (GSCU100C, ProSciTec, Australia) and incubated for 5 min. After removal of excess liquid, the sample was washed twice with MQW to reduce the formation of salt crystals. Negative staining was conducted for 2 min with 2 % w v<sup>-1</sup> uranyl acetate. A FEI Tecnai G2 Spirit with an Olympus SIS Veleta CCD camera was used to obtain images at 120 kV voltage. Particle diameter was measured by counting pixels using GIMP 2.10.18.

### 2.4. High throughput process technology strategies applied for studying binding capacity of resins

Briefly, 96 well PreDicator® (Cytiva, Sweden) plates filled with 20 µl of Capto™ MMC or Capto™ Q were used for high throughput binding screening. The pH values 7.5, 8.0, 8.5 and 9.0 and NaCl concentrations from 0–500 mM were screened. L buffers at the desired pH values, containing 0 M NaCl, were prepared 6 times concentrated as well as 3 M NaCl solution and a VP1-J8 stock solution. The stock solutions were finally mixed in the PreDicator® plate wells to a total volume of 300 µl (50 µl 6x L buffer, 0–50 µl 3 M NaCl, 0–50 µl MQW, 200 µl VP1-stock solution or MQW for equilibration). The protocol followed standard procedure. Solutions in the PreDicator® plates were removed by 2 min centrifugation at 500 g. The wells were equilibrated 3 times with desired buffer (5 min shaking at 1200 rpm). After equilibration, buffer with VP1-J8 stock solution instead of MQW was added and shaken for 60 min at 1200 rpm. The bound VP1-J8 was calculated by measuring the concentration in the unbound samples by HPLC and subtract it from the initial VP1-J8 concentration for loading. The DNA concentration was measured as described and compared to the initial DNA concentration for loading. The experiments were automated using a Microlab® Nimbus4® automated liquid handler (Hamilton,

USA). The results presented here are an average of duplicates (experiments and samples).

VP1-J8 stock solution was prepared by adding PEG-6000 and NaCl to a final concentration of 7 % w v<sup>-1</sup> and 0.5 M respectively to clarified lysate to precipitate the VP1-J8 out. After gently shaking and 10 min incubation on ice, the precipitated VP1-J8 was separated by centrifugation at 20,130 g for 10 min at 4°C. The pellet was washed several times with 5 ml MQW to remove PEG and salts. Thereafter the pellet was resolubilized in 15 ml L buffer containing no buffer salt (MQW, 5 % w w<sup>-1</sup> glycerol, 5 mM DTT, 2 mM EDTA, 1x protease inhibitor) and the pH was readjusted to 8.25. Any undissolved residues were removed by centrifugation for 10 min at 20130 g, 4°C, and filtering through a 0.22 µm filter (16532 Minisart®, Sartorius, Germany).

## 2.5. High throughput elution study

To establish the optimal elution conditions elution studies on 96 well PreDictor® plates filled with 20 µl Capto™ MMC were performed. Elution buffers at pH values of 8, 9, 10, 11, 12 and NaCl concentrations of 0–2 M were examined. Pipetting was done with a Nimbus automated liquid handler (Hamilton, US). L buffers at different pH values were prepared 2 times concentrated, as well as a 4 M NaCl stock solution and mixed to a final volume of 200 µl inside the wells (100 µl 2x L buffer, 0–100 µl 4 M NaCl solution and 0–100 µl MQW). The VP1-J8 stock solution was prepared as described in the previous section, except precipitated VP1-J8 was resolubilized in L buffer pH 8, 0.5 M NaCl (40mM Tris, 5 % w w<sup>-1</sup> glycerol, 5 mM DTT, 2 mM EDTA, 1x protease inhibitor). Predictor plates were equilibrated 3 times for 5 min at 1200 rpm with L buffer pH 8, 0.5 M NaCl and loaded 60 min at 1200 rpm with 200 µl of VP1-J8 stock solution. After loading the wells were washed 3 times at 1200 rpm for 5 min with L buffer pH 8, 0.5 M NaCl containing no DTT, to remove optical interfering substances like oxidized DTT and other impurities. Two elution steps were conducted in which the wells were filled with elution buffers, incubated for 5 min at 1200 rpm and centrifuged for 2 min at 500 g. The Absorbance A<sub>280</sub> of the eluent solution was measured on a 2300 Victor X5 multilabel reader (PerkinElmer, US). The absorbances of both elution steps were added and normalized to the measured maximum. The results presented here are an average of duplicates (experiments and samples).

## 2.6. Dynamic binding capacity

The resin dynamic binding capacity at 10 % breakthrough (DBC<sub>10</sub>) was measured at a flow rate of 0.33 ml min<sup>-1</sup> on a 1 ml pre-packed Capto™ MMC column. VP1-J8 stock solution (VP1-J8 concentration: 2.13 mg<sub>VP1-J8</sub> ml<sup>-1</sup>) at pH 8.9, 0.35 M NaCl, prepared as described by PEG precipitation, was used and loaded onto the column. The flowthrough was collected in 2 ml fractions and the VP1-J8 content determined by RP-HPLC. To verify the results and to test the influence of the starting impurity level or product concentration, purified sample by Capto™ MMC were diluted with L buffer pH 8 and readjusted to pH 8.9, 0.35 M NaCl (VP1-J8 concentration: 0.79 mg<sub>VP1-J8</sub> ml<sup>-1</sup>), fractions were analysed by Bradford assay.

## 2.7. Process integration and further polishing

Several possible purification pathways in which Capto™ MMC is incorporated have been examined as shown in Fig. 1 (pathway A to F). Pathway A and B started with PEG precipitation, followed by Capto™ MMC purification and an additional polishing step, either by SEC or by Capto™ Q. Pathway C and D also started with PEG precipitation, however, followed by Capto™ Q flow through

chromatography and either SEC or Capto™ MMC was used as a third/polishing purification step. Pathway E combined Capto™ Q with Capto™ MMC without a PEG precipitation. Pathway F combined diafiltration with Capto™ MMC.

PEG precipitation was conducted as described in Section 2.4, except the precipitate was resolubilized in L buffer pH 8.9, 0.35 M NaCl. Under this condition VP1-J8 bound strongly to Capto™ MMC and basically did not bind to Capto™ Q. The salt concentration in the load material also minimizes DNA-protein interaction and therefore beneficially influenced the purification process by minimising product loss in the first step. Capto™ Q flow through experiments were done either with a custom-packed column containing 14 ml of resin (XK 16/20 Column, Cytiva, Sweden) or with a 1 ml pre-packed column on an ÄKTA pure system at flow rates of 1 ml min<sup>-1</sup> or 0.33 ml min<sup>-1</sup> respectively with L buffer pH 8.9, 0.35 M NaCl as a running buffer. Samples obtained from Capto™ Q flowthrough, PEG precipitation or clarified lysate were loaded on 1 ml Capto™ MMC with L buffer pH 8.9, 0.35 M NaCl at a flow rate of 0.33 ml min<sup>-1</sup>. Elution from Capto™ MMC was achieved by applying a step gradient with L buffer pH 12, 0 M NaCl at 1 ml min<sup>-1</sup>. In the case in which Capto™ Q flow through purification was performed after Capto™ MMC, the sample was diluted 1:4 with L buffer pH 8 and the pH and NaCl concentration were adjusted to 8.9 and 0.35 M respectively. A Superose®6 (Cytiva, Sweden) column was used for SEC polishing with L buffer pH 8, 0.5 M NaCl at a flow rate of 0.6 ml min<sup>-1</sup>. For batch diafiltration 15 ml Amicon® Ultra-15 centrifugal filter units with a molecular weight cut-off of 100 kDa were used (UFC9100, MilliporeSigma, USA). A sample of 15 ml crude lysate (pH 8.9, 0.35 M NaCl) was centrifuged at 5000 g till the volume reached 2 ml. It was then diluted 1:1 with L buffer pH 8.9 0.35 M NaCl, and centrifuged till a volume of 2 ml. This step was repeated 5 times and it took about 8 h.

## 2.8. Virus-like particle assembly

Purified VP1-J8 capsomeres were assembled by adding calcium chloride directly into the protein solution, based on a method described by Liew et al. [46].

Purified VP1-J8 capsomeres were obtained as described in Table 1 pathway E. Clarified supernatant was purified on Capto™ Q in flow through mode (pH 8.9, 0.35 M NaCl) and without further buffer adjustment loaded onto a 1 ml Capto™ MMC column. After loading, the column was washed for 10 CV with washing buffer without DTT (20mM Tris, 5 % w w<sup>-1</sup> glycerol, 1 mM EDTA, 0.35 M NaCl, pH 8.9) and step eluted with a sodium hydrogen orthophosphate buffer at pH 12 containing 1 M NaCl (20mM sodium hydrogen orthophosphate, 5 % w w<sup>-1</sup> glycerol, 1 mM EDTA, 1 M NaCl, pH 12). The increased NaCl was chosen as it supports VLP assembly. The eluate was diluted with elution buffer to a VP1-J8 concentration of 0.6 mg ml<sup>-1</sup> and pH adjusted to pH 7.2 with HCl. After pH adjustment 100 mM CaCl<sub>2</sub> stock solution was added to a final concentration of 3 mM CaCl<sub>2</sub> and subsequently incubated for 12h at room temperature. The solution was analysed by TEM as described in Section 2.3.

## 3. Results

### 3.1. High throughput binding studies

Figs. 2 and 3 show contour plots of the static binding of VP1-J8 on Capto™ Q and Capto™ MMC resins, respectively. Fig. 4 shows bound DNA on Capto™ Q expressed as percent of the loaded DNA. Values in the figures are rounded to the closest colour level. For Capto™ MMC initially 29.1 mg VP1-J8 per ml resin was loaded, and for Capto™ Q 53.5 mg VP1-J8 per ml resin. In general, VP1-J8 showed poor binding affinity towards Capto™ Q at all examined

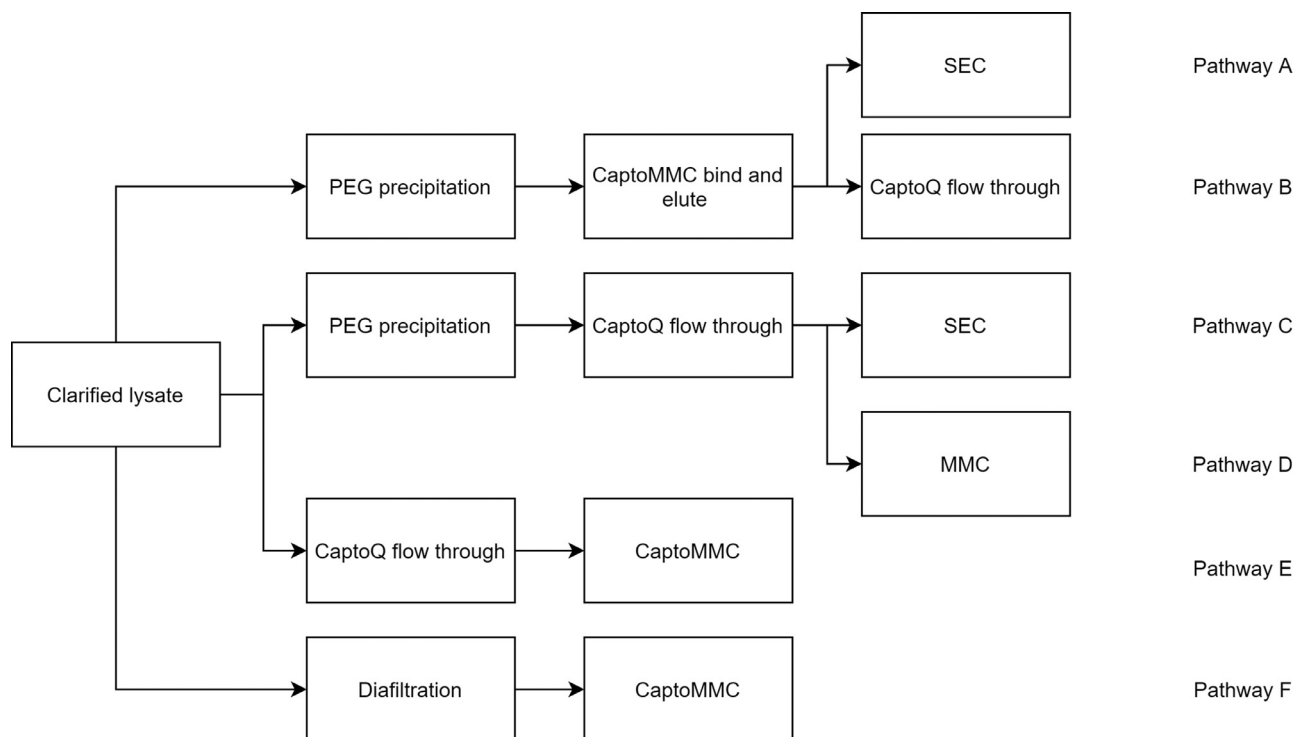


Fig. 1. Possible purification pathways examined in this research.

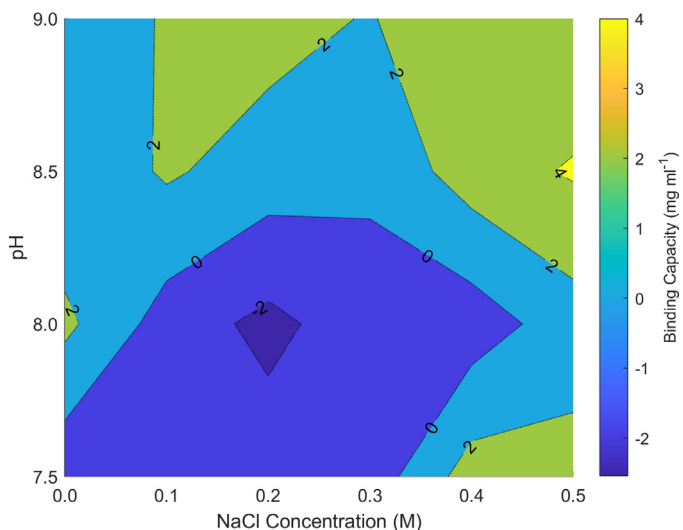


Fig. 2. Static binding of VP1-J8 on Capto™ Q measured with 20  $\mu$ l PreDicator® plates in the range pH 7.5–9.0 and NaCl 0–0.5 M.

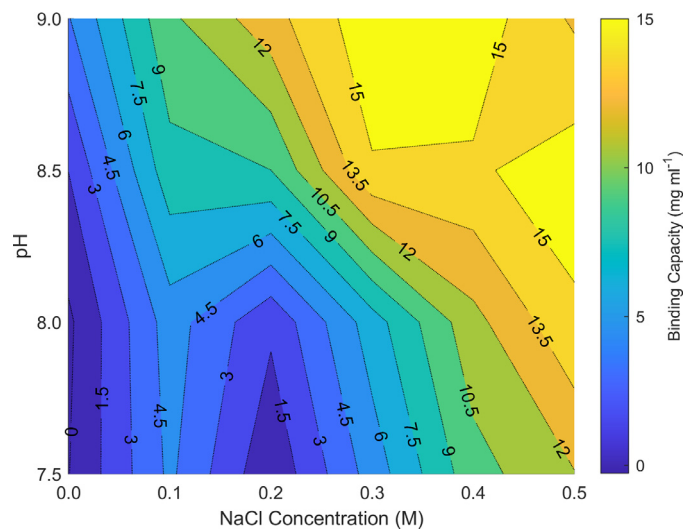


Fig. 3. Static binding of VP1-J8 on Capto™ MMC measured with 20  $\mu$ l PreDicator® plates in the range pH 7.5–9.0 and NaCl 0–0.5 M.

conditions with a maximum measured binding capacity of 4.2  $\text{mg ml}^{-1}$  at pH 8.5, 0.5 M NaCl and capacities ranging from -1.4 to 3.8  $\text{mg ml}^{-1}$  at the other conditions. The negative value might be derived from measurement uncertainty, due to the high concentration of loaded material. Therefore, negative values should not be considered in this instance. The binding capacity slightly increased with increasing NaCl concentration. DNA binding on Capto™ Q was low if no NaCl was present in the buffer (< 5 % for pH 7.5–8.5, and 15 % at pH 9.0, 0 M NaCl in each case) and increased with increasing NaCl concentrations, eventually reaching an optimum at 0.3 M NaCl and decreased at higher NaCl concentrations. The highest DNA binding was measured at pH 7.5 at NaCl concentrations

between 0.3 and 0.4 M, at which 38 % of the loaded DNA bound to the resin, as shown in Fig. 4.

In contrast, VP1-J8 showed a strong binding towards Capto™ MMC at elevated NaCl concentrations. The highest binding capacity was measured at pH 9, 0.3 M NaCl with 16.0  $\text{mg ml}^{-1}$  and binding at 0 M NaCl was below 4  $\text{mg ml}^{-1}$  at all pH values. There is a clear trend that VP1-J8 poorly binds to Capto™ MMC at low salt concentrations and starts binding with increasing NaCl concentrations. This effect is also pH dependent. While at pH 7.5, 0.4 M NaCl is required to obtain a binding capacity of 10  $\text{mg ml}^{-1}$ , only 0.2 M NaCl is required at pH 9. The binding shows an optimum at a certain NaCl concentration and at higher NaCl binding decreases.

**Table 1**

Different examined purification pathways. HMWli: High molecular weight impurities, LMWli: Low molecular weight impurities, Aggr: Aggregates, DNA: DNA content, NA: Not applicable if measurement was not expedient.

Pathway A	PEG precipitation	Capto™ MMC	SFC
Pathway B	HMWli: NA, LMWli: NA, Aggr: NA, DNA: 29.7 µg mg <sup>-1</sup> PEG precipitation	HMWli: 17.9 %, LMWli: 2.7 %, Aggr: 0.6 %, DNA: 0.38 µg mg <sup>-1</sup> Capto™ MMC	HMWli: 7.0 %, LMWli: 1.1 %, Aggr: 0 %, DNA: 0.04 µg mg <sup>-1</sup> Capto™ Q
Pathway C	HMWli: NA, LMWli: NA, Aggr: NA, DNA: 29.7 µg mg <sup>-1</sup> PEG precipitation	HMWli: 17.9 %, LMWli: 2.7 %, Aggr: 0.6 %, DNA: 0.38 µg mg <sup>-1</sup> Capto™ Q	HMWli: 4.2 %, LMWli: 2.8 %, Aggr: 0 %, DNA: 0.02 µg mg <sup>-1</sup> SFC
Pathway D	HMWli: NA, LMWli: NA, Aggr: NA, DNA: 29.7 µg mg <sup>-1</sup> PEG precipitation	HMWli: 25.2 %, LMWli: 3.6 %, Aggr: 3.1 %, DNA: 0.04 µg mg <sup>-1</sup> Capto™ Q	HMWli: 18.1 %, LMWli: 1.5 %, Aggr: 0 %, DNA: 0.01 µg mg <sup>-1</sup> Capto™ MMC
Pathway E	HMWli: 42.7 %, LMWli: 22.9 %, Aggr: 2.8 %, DNA: 0.02 µg mg <sup>-1</sup> Capto™ Q	HMWli: 25.2 %, LMWli: 3.6 %, Aggr: 3.1 %, DNA: 0.04 µg mg <sup>-1</sup> Capto™ MMC	HMWli: 2.1 %, LMWli: 1.5 %, Aggr: 0 %, DNA: 0.04 µg mg <sup>-1</sup>
Pathway F	HMWli: 50.3 %, LMWli: 29.0 %, Aggr: NA, DNA: 23.61 µg mg <sup>-1</sup> Diafiltration	HMWli: 10.9 %, LMWli: 1.7 %, Aggr: 0 %, DNA: 0.004 µg mg <sup>-1</sup> Capto™ MMC	
		HMWli: 50.0 %, LMWli: 1.1 %, Aggr: 1.46 %, DNA: 1.85 µg mg <sup>-1</sup>	

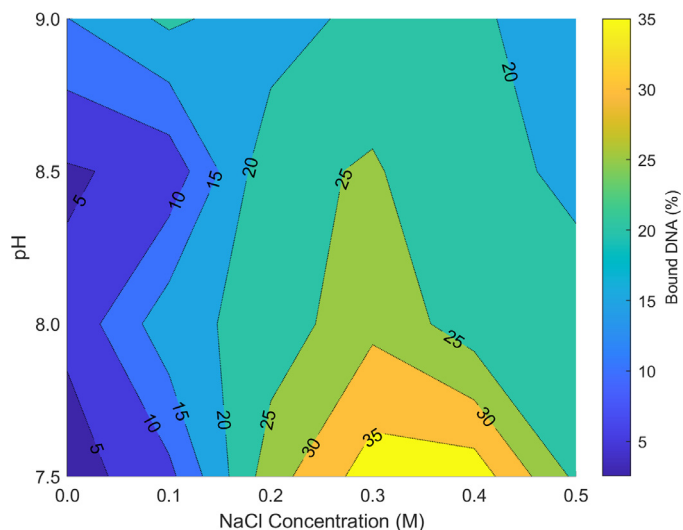


**Fig. 4.** Bound DNA on Capto™ Q during static binding studies with 20 µl PreDicator® plates in the range pH 7.5–9.0 and NaCl 0–0.5 M. Bound DNA is expressed as percentage of initial DNA loaded onto the resin.

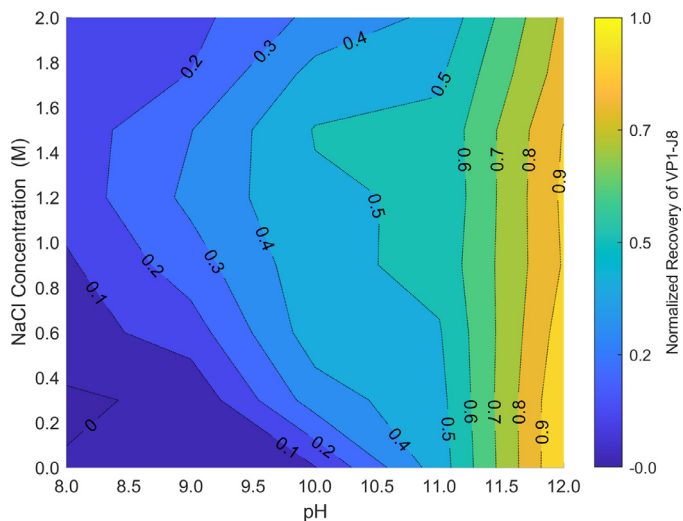


**Fig. 5.** Elution study of VP1-J8 from Capto™ MMC for a pH range from 8–12 and NaCl concentrations from 0–2 M. Cumulative recovery obtained from 2 consecutive steps normalized to the maximum.

For example, maximum binding at pH 9 is at 0.3 M NaCl (16.0 mg ml<sup>-1</sup>) and at 0.5 M NaCl it decreased to 13.2 mg ml<sup>-1</sup>.

**3.2. High throughput elution studies**

The best elution from Capto™ MMC was observed at pH 12, 0 M NaCl, and no elution was measured at pH values and NaCl concentrations below the loading condition (pH 8, 0.5 M NaCl). As can be seen as a general trend in Fig. 5, increasing NaCl concentration led to better elution with a maximum at around 1.2–1.4 M NaCl. At higher salt concentrations however, VP1-J8 elutes less. This trend is only true for pH values below 12, as at pH 12 the strongest elution is at 0 M NaCl. Increasing NaCl concentration led to lower elution, but still high, compared to other elution conditions tested. Rising pH supports elution gradually at all NaCl concentrations and showed a steep increase from pH 11 to 12.

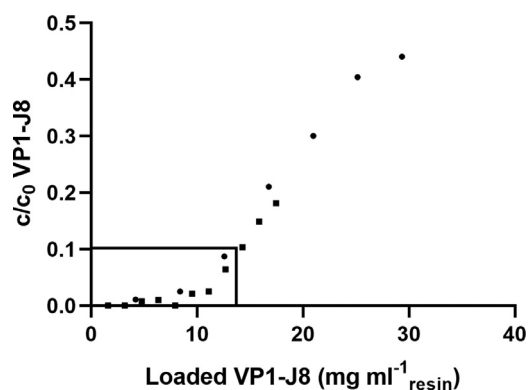


**Fig. 6.** Breakthrough curve of VP1-J8 on a 1 ml Capto™ MMC column at pH 8.9, 0.35 M NaCl at a flow rate of 1 ml min<sup>-1</sup>. The marked square indicates a DBC<sub>10%</sub>. (•) VP1-J8 stock solution, obtained by PEG precipitation. (■) Purified VP1-J8.

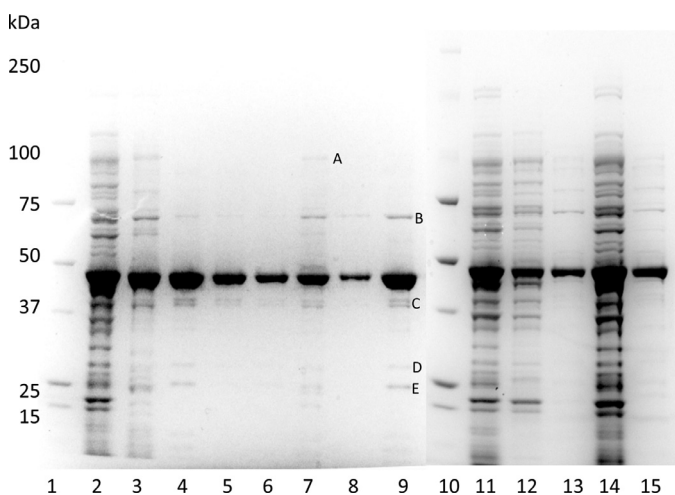


**Fig. 7.** SDS-PAGE analysis of purification pathways A-F as described in Fig. 1. (1 & 10) Marker, (2) clarified cell lysate, (3) resolubilized PEG precipitate (pathway A & B), (4) PEG followed by Capto™ MMC (pathway A & B), (5) SEC polishing (pathway A), (6) Capto™ Q polishing (pathway B), (7) PEG precipitation followed by Capto™ Q flow through (pathway C & D), (8) SEC polishing (pathway C), (9) Capto™ MMC polishing (pathway D), (11) clarified cell lysate, (12) Capto™ Q flow through of clarified cell lysate (pathway E), (13) Capto™ MMC polishing (pathway E), (14) retentate of diafiltration (pathway F), (15) Capto™ MMC polishing (pathway F). Protein identity of impurities A-E were analysed by LC-ESI-MS/MS Mass Spectrometry.

### 3.3. Dynamic binding capacity

As can be seen in Fig. 6, the purity and concentration of the starting material had a negligible influence on dynamic binding capacity. Both experiments showed a DBC<sub>10%</sub> of around 14 mg ml<sup>-1</sup> resin at a residence time of 1 min for VP1-J8 on Capto™ MMC. The dynamic binding is comparable to high throughput results, but in this case slightly lower, to the static binding measured with high throughput binding studies in which a binding of 15–16 mg ml<sup>-1</sup> was obtained for the chosen buffer conditions.

### 3.4. Process integration and further polishing

Although the binding of VP1-J8 on Capto™ MMC at a pH above 8 seems to be highly specific it was found that purification by Capto™ MMC alone does not result in a pure product.

The purity analysis of the different purification pathways is summarized in Table 1. The results of SDS-PAGE analysis are shown in Fig. 7. Purity analysis by size exclusion methods of the products obtained by PEG precipitation and diafiltration was not expedient

as the impurity levels, in particular DNA levels, were too high and therefore distorted the results.

PEG precipitation followed by Capto™ MMC purification led to SEC purities of around 80 % and removed the majority of DNA. Very low levels of aggregates (0.6 %) could be measured, however the identity of the aggregates could not be verified as VP1-J8 aggregates. Both subsequent polishing steps, either by size exclusion chromatography or by flow through polishing on Capto™ Q further increased the purity to levels above 90 % and DNA levels below 0.04 μg mg<sub>protein</sub><sup>-1</sup>. No aggregates could be detected after polishing.

PEG precipitation followed by Capto™ Q flow through purification lowered DNA levels to 0.04 μg mg<sub>protein</sub><sup>-1</sup>, and achieved a SEC purity of around 70 %. Around 3.1 % VP1-J8 aggregates were present in the sample. Polishing by SEC led to the removal of aggregates, however HMWI remained high with 18.1 %. Polishing with Capto™ MMC removed aggregates and also removed most of the HMWI (HMWI: 2.1 %).

The combination of AEX flowthrough followed by Capto™ MMC purification, without a prior PEG precipitation step, showed similar results, with slightly higher impurities. After the flow through step the DNA level was very low, but VP1-J8 aggregates were present (2.8 % aggregates). HMWI (42.7 %) and LMWI (22.9 %) were higher than with a prior PEG precipitation step (HMWI: 25.2 %, LMWI: 3.6 %). The subsequent Capto™ MMC step strongly reduced HMWI and LMWI impurities to 10.9 % and 1.7 % respectively, and aggregates could not be detected. The remaining DNA content of 0.004 μg mg<sub>protein</sub><sup>-1</sup> was the lowest measured for all purification steps and is below the detection limit of the assay.

Diafiltration as an alternative first purification step resulted in insufficient outcomes. DNA levels could not be lowered in the diafiltration step and impurity levels remained high. Also the subsequent Capto™ MMC step showed poor performance and very high HMWI impurities of 50.0 % remained. Furthermore 14.6 % aggregates could be measured and DNA at a comparable very high level of 1.85 μg mg<sub>protein</sub><sup>-1</sup> was present. Nonetheless, the aggregates could not be identified by SDS-PAGE as VP1-J8 aggregates or any other protein and a comparison of the A<sub>260</sub>/A<sub>280</sub> ratio of 1.96 indicates that the measured aggregate fraction is in fact nucleic acid (data not shown).

SDS-PAGE analysis confirms the SEC-HPLC analysis. PEG precipitation, Capto™ Q and Capto™ MMC are possible unit operations to purify VP1-J8. PEG precipitation and Capto™ Q did not result in pure product (Fig. 7, line 3, 7, 12). In combination with Capto™ MMC the purity is very high. The Capto™ MMC step in particular showed a high specificity towards VP1-J8 and thus strongly increased the purity. This is especially evident for the purification after diafiltration (Fig. 7, line 14 & 15). The combination of Capto™ Q and Capto™ MMC lead to a product of high purity, with only faint bands of impurities visible (Fig. 7 lane 9 & 13, impurities A-E). These impurity bands could not be removed in our experiments and become visible if the SDS gel was overloaded. However, the pathway without prior PEG precipitation showed slightly higher impurities for proteins > 50 kDa (Fig. 7, lane 13) and lower impurities for proteins < 50 kDa. Impurity A has a molecular weight of around 90 kDa, impurity B of around 70 kDa, impurity C shows a double band at around 40 kDa and impurity D & E has a molecular weight of 25 & 20 kDa, respectively. Protein identification by comparing protein fingerprints of the impurity bands via LC-ESI-MS/MS as described in Section 2.3 against *E.coli* proteins and VP1-J8 revealed that impurities C, D and E showed the highest coverage with VP1-J8. Impurity C had a coverage of 69 %, impurity D of 57 % and impurity E of 59 %. Known *E. coli* proteins showed a significantly lower coverage. As impurities C, D and E have a lower molecule weight as native VP1-J8 but showed a high fingerprint coverage of VP1-J8, it can be concluded that impurities C, D and E



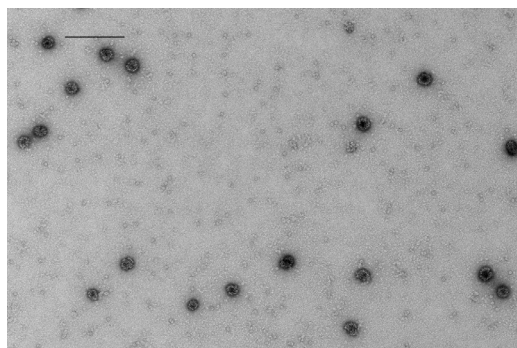


**Fig. 8.** TEM image of VLPs assembled by lowering the pH to 7.2 and adding calcium chloride to the eluate obtained from pathway E. Scale bar represents 200 nm.

are truncation products of VP1-J8. Unfortunately, Impurities A and B showed no signal in LC-ESI-MS/MS at all and therefore could not be identified (below detection limit).

### 3.5. VLP assembly

As can be seen in Fig. 8 the capsomeres from pathway E (Fig. 1) could be successfully assembled into capsid like structures by solely lowering the pH and adding calcium chloride. The measured diameters of the particles ranged from 42 nm to 52 nm. Apart from capsid like structures also unassembled capsomeres were visible on the TEM images but no spherical aggregates between 15 and 30 nm.

## 4. Discussion

At a pH range from 7.5 to 9.0 VP1-J8 capsomeres showed static binding capacities between  $-1.4$  to  $3.8 \text{ mg ml}_{\text{resin}}^{-1}$  on Capto<sup>TM</sup> Q. Keeping in mind that at the high concentration used in these tests, 1 % error in the concentration determination corresponds to around  $0.5 \text{ mg ml}_{\text{resin}}^{-1}$  difference in binding capacity it can be concluded, that VP1-J8 capsomeres do not effectively bind Capto<sup>TM</sup> Q. This result is unexpected given the fact that VP1-J8 has a theoretical isoelectric point of 6.57 and should therefore have an overall negative charge and expected to bind to strong anion exchangers for selected buffer systems. It is also contrary to reports in the literature in which VP1 capsomeres have been captured on Sartobind® Q membranes at pH 8 having the same ligand [41]. The slightly increased binding at elevated NaCl concentrations, can be explained by non-specific hydrophobic interactions. In contrast, VP1-J8 does bind strongly towards Capto<sup>TM</sup> MMC, a mixed mode cation exchanger, at the examined pH range for elevated NaCl concentrations but with only low levels at low salt concentrations. For a given NaCl concentration (e.g. 0.3 M NaCl) the binding capacity actually increases with increasing pH. This behaviour is somewhat strange, and a plausible explanation would be that hydrophobic interactions are the predominant binding mechanism between Capto<sup>TM</sup> MMC and VP1-J8. However, that would also mean that VP1-J8 binding increases with increasing salt concentrations [48]. As the binding capacity decreases again at high salt concentrations (see Fig. 3 pH 9, 0.5 M NaCl) this explanation seems to be untrue. Furthermore, the measured optimal salt concentrations (0.3–0.5 M NaCl) are far below reported concentrations in which hydrophobic effects play a dominant role at mixed mode cation exchangers [48]. The elution experiments strengthen the assumption that the binding mechanism is in fact an electrostatic binding. At salt concentrations down to 0 M NaCl VP1-J8 does not elute from Capto<sup>TM</sup> MMC, which is contrary to the observations made during binding studies, in which VP1-J8 does poorly bind at this condition. If hydrophobic

interactions are responsible for the binding it would be expected to show some elution at very low salt concentrations which cannot be observed [48]. The elution behaviour with a maximum elution at salt concentrations around 1.4 M NaCl and lower elution at higher salt concentrations shows that hydrophobic effects only play a dominant role at very high salt concentrations. Increasing the pH beneficially affects the elution as expected and as described by the manufacturer [49]. At a high pH value of 12 binding strongly decreased at all salt concentrations having the highest elution at 0 M NaCl. This might be explained by that fact that ionic binding occurs at a charged patch, rather than by the overall net charge of the protein. A possible binding site is the exposed N-terminal DNA binding site of VP1, which is rich in arginine and lysine, having pKa's of 12.48 and 10.53, respectively [50].

Assuming that the binding is predominantly caused by localised electrostatic interactions, the binding behaviour still opens questions. Comparing the binding of VP1-J8 on Capto<sup>TM</sup> MMC with the binding of DNA onto Capto<sup>TM</sup> Q the similarities are obvious. As shown in literature DNA binds to anion exchangers such as Capto<sup>TM</sup> Q especially well at low ionic strengths [51]. However, at low ionic strengths neither DNA on Capto<sup>TM</sup> Q nor VP1-J8 on Capto<sup>TM</sup> MMC bind properly on the resin and binding increased with increasing NaCl concentrations; a phenomenon between the two types of interactions are evident. We could show that VP1-J8 is forming soluble DNA-protein aggregates at low ionic strengths, caused by the strong DNA binding site on VP1 subunits, which effectively hinders VP1-J8 of accessing the pores of chromatographic resin and thus lead to very low binding capacities at low ionic strengths (results submitted to publication). At salt concentrations having an optimum binding (0.3–0.4 M NaCl) the ionic strength leads to dissociation of DNA-protein complexes, but due to the salt tolerance of Capto<sup>TM</sup> MMC, only minimally affect the overall binding capacity. This effect explains the divergence between binding and eluting at low ionic strengths, the overall binding behaviour and also explains why DNA cannot be properly removed on Capto<sup>TM</sup> Q at low ionic strengths. Combining the data, it can be concluded that processing of VP1-J8 requires a NaCl above 0.3 M NaCl. Optimal loading conditions on Capto<sup>TM</sup> MMC are NaCl concentrations between 0.3 and 0.4 at pH values above 8.5 and for DNA removal on Capto<sup>TM</sup> Q a pH of 7.5 should be chosen, but also higher pH values are applicable. Preferable elution conditions are at pH 12 at low ionic strengths, but NaCl can be added in concentrations up to 2 M with only minimal negative effects on elution.

The optimal elution conditions at a pH of 12 are generally considered as very harsh and should be avoided in protein processing as proteins at very high pH values might degenerate over time due to micro chemical changes. These reactions are favoured by long exposure time and high temperatures [52]. However, such harsh conditions are only used for a few minutes during elution and could be neutralized immediately. Therefore, it can be assumed that the degeneration is minimal. This is also supported by the fact that the acquired capsomeres show no abnormal behaviour compared to capsomeres obtained without a high pH elution step (e.g. pathway C, data not shown). Alternatively, as many other mixed mode ligands than Capto<sup>TM</sup> MMC exist, a broad screening likely will find a ligand with enhanced elution at lower pH values [53].

The measured dynamic binding capacity was nearly independent from product concentration and product purity. Thus, a Capto<sup>TM</sup> MMC purification step can be used at every step during purification without any negative impact on the performance. Although, the measured DBC<sub>10%</sub> of  $14 \text{ mg ml}^{-1}$  is significantly lower than reported DBCs for e.g. BSA on Capto<sup>TM</sup> MMC ( $30 \text{ mg ml}^{-1}$ ) [54], the capacity is comparable to highly overloaded affinity ligands (GSTrap HP,  $22 \text{ mg ml}^{-1}$ ) [37] and far higher than reported dynamic binding capacities of  $5.7 \text{ mg ml}^{-1}$  for human B19 parvovirus-like particles on Sartobind® Q [55].

The obtained design space allows the construction of several purification pathways, of which a few have been examined. As expected, a three-step purification (pathway A–D) with capturing by selective precipitation leads to higher purities compared to a two-step purification (pathway E & F). Surprisingly, VP1-J8 aggregates seem not bind to Capto™ MMC as can be clearly seen in pathway E and D. This is unexpected as usually, even after an affinity purification step, aggregates are present and must be subsequently separated by SEC [56]. Steric hindrance of the aggregates might be an explanation; another rationale could be that the binding site might be inaccessible in aggregated form. Although the mechanism is unknown, purification by Capto™ MMC eradicates the need for a size exclusion step, which is an expensive purification step.

Selective precipitation is a valuable process for lab scale purification, however, the scale-up raises issues, as the resolubilisation of the precipitate is challenging at large scale, especially if captured by centrifugation, which compresses the pellet and therefore hinders the resolubilisation [57]. Diafiltration, although widely used in industry for initial purification of VLPs, was impractical as an alternative to precipitation as it showed low removal of impurities, lead to aggregation of the product and proved to be very time consuming. Tangential flow filtration might increase the performance but was not tested. The two-step purification pathway (pathway E), without PEG precipitation, consisting of a Capto™ Q flow through step followed by a Capto™ MMC bind and elute step, showed similar process characteristics as pathway D. Aggregates and DNA are completely removed and SEC-HPLC purities close to 90 % are achieved. Furthermore, less truncation product could be identified, which might be a result of the faster processing compared to the three-step pathway. If higher purities are required, new multi modal size exclusion resins such as Capto™ Core™ might be a promising approach that yet has to be tested.

Using a flow through step on as an initial purification step is rather unusual, but in our process has the advantages of a direct subsequent loading onto Capto™ MMC without any buffer adjustment and therefore eradicates a unit operation. It also reduces the impurity level to a point at which the Capto™ MMC loading step can be controlled by the UV signal, which is impossible if crude lysate is loaded. This comes, however, at the cost of higher resin costs, as more resin is needed compared to a flow through polishing step. The eluate obtained from Capto™ MMC can be directly assembled into well-formed VLPs by just lowering the pH and adding calcium ions to the solution; no aggregates or miss formed VLPs could be identified. As expected a small amount of capsomeres remained unassembled, an effect already described in the literature, which is negatively correlated to the concentration during assembly [58]. A higher initial concentration can be easily achieved as VP1-J8 is eluted highly concentrated, which will lead to higher recoveries during assembly. Although the overall product recovery has not been evaluated, the process shows no intrinsic product loss and therefore likely has a very high recovery. Compared to other described processes in the literature for the production of viral capsomeres and VLPs our process has several advantages and address some of the common bottlenecks like benzonase treatment for DNA removal, removal of affinity tags, protein refolding, density gradient centrifugation, the use of SEC, multiple buffer exchanges, or the use of low capacity membrane columns [34,35,41,59]. Furthermore, the process is fully scalable, easy to integrate and rapid, as the purification is completed in less than 3 hours. The obtained VLPs are also already highly concentrated in PBS buffer containing only VLPs, capsomeres, EDTA, glycerol and NaCl at a physiological pH value, thus formulation can be achieved by solely diluting it to the required concentration.

Several VP1-J8 truncation products could be identified on SDS-PAGE analysis at purified samples. Although it was not possible to identify impurities A and B, it is likely that they are chaperones

that bound to VP1-J8. Having a size of around 70 kDa, impurity B is probably the prokaryotic hsp70 chaperone DnaK, which was shown to copurify with VP1 [60] and impurity A is hsp90 which interacts with hsp70 [61]. Another possibility is the formation of inter-polypeptide aggregates of VP1-J8 and VP1-J8 truncation products during SDS sample preparation by partial reoxidation [62]. The double band on SDS-PAGE gels at 43 & 40 kDa have already been described in literature and occur due to auto digestion of VP1, as VP1 has an intrinsic serine protease activity [63]. As SEC-HPLC still reveals a near uniform capsomere peak we conclude, that partially digested VP1-J8 still remains in pentameric form together with intact VP1-J8 monomers and therefore are impossible to remove. The formation of truncation products of viral protein during the expression in *E. coli* has also been reported for adeno associated viral protein VP3 and might therefore also be a result of *E. coli* proteases [28]. Further research needs to be undertaken to minimize the formation of these digestion products, and how to remove the bound chaperones, but using protease inhibitors throughout the whole process instead of only during cell disruption, run at reduced temperature and addition of ATP to remove chaperones will likely solve the issue.

## 5. Conclusion

In this study we developed a robust and theoretically fully scalable, highly efficient process for the production of modular murine polyomavirus major structural protein VP1-J8 capsomeres and modular VLPs using high-throughput process development tools. Purification by mixed mode cation exchanger at pH values above 8 showed a highly specific binding and dynamic binding of 14 mg ml<sup>-1</sup> resin<sup>-1</sup> was achieved under the optimised conditions. The developed two step purification pathway, consisting of an anion exchange flow through step followed by a bind and elute step on a multimodal cation exchanger, requires no buffer adjustment during processing and is thus incomparably simple and fast. The developed process removes the majority of host cell protein, aggregates and DNA, without any of the common bottleneck unit operations in other described VLP production pathways. VLPs in PBS buffer can be obtained by simply adding calcium ions to the final eluate and lowering the pH to 7.2. This straightforward process, requiring only three integrated unit operations might lay the baseline for future cost effective, large scale production of microbial produced modular VLP vaccine candidates.

## Declaration of Competing Interest

The authors declare that they have no known competing financial interests or personal relationships that could have appeared to influence the work reported in this paper.

## CRedit authorship contribution statement

**Lukas Gerstweiler:** Conceptualization, Methodology, Investigation, Writing - original draft, Visualization. **Jagan Billakanti:** Conceptualization, Methodology, Writing - review & editing. **Jingxiu Bi:** Conceptualization, Resources, Writing - review & editing, Supervision. **Anton Middelberg:** Conceptualization, Resources, Writing - review & editing, Supervision, Project administration.

## Acknowledgment

The authors thank Ms Ruth Wang for technical support for LC-ESI-MS/MS and the Protein Expression Facility of the University of Queensland, Brisbane, Australia for plasmid construction.

## Supplementary materials

Supplementary material associated with this article can be found, in the online version, at [doi:10.1016/j.chroma.2021.461924](https://doi.org/10.1016/j.chroma.2021.461924).

## References

- [1] S.L. Cochi, L. Hegg, A. Kaur, C. Pandak, H. Jafari, The global polio eradication initiative: progress, lessons learned, and polio legacy transition planning, *Health Affairs* 35 (2016) 277–283, doi:10.1377/hlthaff.2015.1104.
- [2] WHO, Measels fact sheet, 2019. <https://www.who.int/news-room/fact-sheets/detail/measles> (accessed 16 September 2020).
- [3] G. Yamey, M. Schäferhoff, R. Hatchett, M. Pate, F. Zhao, K.K. McDade, Ensuring global access to COVID-19 vaccines, *Lancet* 395 (2020) 1405–1406, doi:10.1016/S0140-6736(20)30763-7.
- [4] M. Rahi, A. Sharma, Mass vaccination against COVID-19 may require replays of the polio vaccination drives, *EclinicalMedicine* 25 (2020) 100501, doi:10.1016/j.eclinm.2020.100501.
- [5] S. Luby, R. Arthur, Risk and response to biological catastrophe in lower income countries, *Curr. Top. Microbiol. Immunol.* 424 (2019) 85–105, doi:10.1007/82\_2019\_162.
- [6] T.R. Doel, FMD vaccines, *Virus Res.* 91 (2003) 81–99, doi:10.1016/S0168-1702(02)00261-7.
- [7] F. Krammer, R. Grabherr, Alternative influenza vaccines made by insect cells, *Trends Mol. Med.* 16 (2010) 313–320, doi:10.1016/j.molmed.2010.05.002.
- [8] B. Donaldson, Z. Lateef, G.F. Walker, S.L. Young, V.K. Ward, Virus-like particle vaccines: immunology and formulation for clinical translation, *Expert Rev. Vaccines* 17 (2018) 833–849, doi:10.1080/14760584.2018.1516552.
- [9] M.A. Stanley, Human papillomavirus vaccines, *Rev. Med. Virol.* 16 (2006) 139–149, doi:10.1002/rmv.498.
- [10] A.P.J. Middelberg, T. Rivera-Hernandez, N. Wibowo, L.H.L. Lua, Y. Fan, G. Magor, C. Chang, Y.P. Chuan, M.F. Good, M.R. Batzloff, A microbial platform for rapid and low-cost virus-like particle and capsomere vaccines, *Vaccine* 29 (2011) 7154–7162, doi:10.1016/j.vaccine.2011.05.075.
- [11] H.K. Hume, J. Vidigal, M.J.T. Carrondo, A.P.J. Middelberg, A. Roldão, L.H.L. Lua, Synthetic biology for bioengineering virus-like particle vaccines, *Biotechnol. Bioeng.* 116 (2019) 919–935, doi:10.1002/bit.26890.
- [12] A. Tekewe, Y. Fan, E. Tan, A.P.J. Middelberg, L.H.L. Lua, Integrated molecular and bioprocess engineering for bacterially produced immunogenic modular virus-like particle vaccine displaying 18 kDa rotavirus antigen, *Biotechnol. Bioeng.* 114 (2017) 397–406, doi:10.1002/bit.26068.
- [13] A. Seth, I.G. Kong, S.-H. Lee, J.-Y. Yang, Y.-S. Lee, Y. Kim, N. Wibowo, A.P.J. Middelberg, L.H.L. Lua, M.-N. Kweon, Modular virus-like particles for sublingual vaccination against group A streptococcus, *Vaccine* 34 (2016) 6472–6480, doi:10.1016/j.vaccine.2016.11.008.
- [14] T. Rivera-Hernandez, J. Hartas, Y. Wu, Y.P. Chuan, L.H.L. Lua, M. Good, M.R. Batzloff, A.P.J. Middelberg, Self-advancing modular virus-like particles for mucosal vaccination against group A streptococcus (GAS), *Vaccine* 31 (2013) 1950–1955, doi:10.1016/j.vaccine.2013.02.013.
- [15] M.R. Anggraeni, N.K. Connors, Y. Wu, Y.P. Chuan, L.H.L. Lua, A.P.J. Middelberg, Sensitivity of immune response quality to influenza helix 190 antigen structure displayed on a modular virus-like particle, *Vaccine* 31 (2013) 4428–4435, doi:10.1016/j.vaccine.2013.06.087.
- [16] C.L. Effio, J. Hubbuch, Next generation vaccines and vectors: designing downstream processes for recombinant protein-based virus-like particles, *Biotechnol. J.* 10 (2015) 715–727, doi:10.1002/biot.201400392.
- [17] V. Qendri, J.A. Bogaards, J. Berkhof, Pricing of HPV vaccines in European tender-based settings, *Eur. J. Health Econ.* 20 (2019) 271–280, doi:10.1007/s10198-018-0996-9.
- [18] A. Zeltins, Construction and characterization of virus-like particles: a review, *Mol. Biotechnol.* 53 (2013) 92–107, doi:10.1007/s12033-012-9598-4.
- [19] D.I. Lipin, Y.P. Chuan, L.H.L. Lua, A.P.J. Middelberg, Encapsulation of DNA and non-viral protein changes the structure of murine polyomavirus virus-like particles, *Arch. Virol.* 153 (2008) 2027–2039, doi:10.1007/s00705-008-0220-9.
- [20] L.K. Pattenden, A.P.J. Middelberg, M. Niebert, D.I. Lipin, Towards the preparative and large-scale precision manufacture of virus-like particles, *Trends Biotechnol.* 23 (2005) 523–529, doi:10.1016/j.tibtech.2005.07.011.
- [21] Y.P. Chuan, Y.Y. Fan, L.H.L. Lua, A.P.J. Middelberg, Virus assembly occurs following a pH- or Ca<sup>2+</sup>-triggered switch in the thermodynamic attraction between structural protein capsomers, *J. R. Soc. Interface* 7 (2010) 409–421, doi:10.1098/rsif.2009.0175.
- [22] L.H.L. Lua, N.K. Connors, F. Sainsbury, Y.P. Chuan, N. Wibowo, A.P.J. Middelberg, Bioengineering virus-like particles as vaccines, *Biotechnol. Bioeng.* 111 (2014) 425–440, doi:10.1002/bit.25159.
- [23] Y.P. Chuan, N. Wibowo, L.H.L. Lua, A.P.J. Middelberg, The economics of virus-like particle and capsomere vaccines, *Biochem. Eng. J.* 90 (2014) 255–263, doi:10.1016/j.bej.2014.06.005.
- [24] A. Roldão, M.C.M. Mellado, L.R. Castilho, M.J.T. Carrondo, P.M. Alves, Virus-like particles in vaccine development, *Expert Rev. Vaccines* 9 (2010) 1149–1176, doi:10.1586/erv.10.115.
- [25] X. Huang, X. Wang, J. Zhang, N. Xia, Q. Zhao, *Escherichia coli*-derived virus-like particles in vaccine development, *NPJ Vaccines* 2 (2017) 3, doi:10.1038/s41541-017-0006-8.
- [26] WHO, Weekly epidemiological record: No. 29, 2014, 89, 321–336, 2014. [https://www.who.int/vaccine\\_safety/committee/reports/wer8929.pdf](https://www.who.int/vaccine_safety/committee/reports/wer8929.pdf) (accessed 17 September 2020).
- [27] Y.-M. Hu, S.-J. Huang, K. Chu, T. Wu, Z.-Z. Wang, C.-L. Yang, J.-P. Cai, H.-M. Jiang, Y.-J. Wang, M. Guo, X.-H. Liu, H.-J. Huang, F.-C. Zhu, J. Zhang, N.-S. Xia, Safety of an *Escherichia coli*-expressed bivalent human papillomavirus (types 16 and 18) L1 virus-like particle vaccine: an open-label phase I clinical trial, *Hum. Vaccin. Immunother.* 10 (2014) 469–475, doi:10.4161/hv.26846.
- [28] D.T. Le, M.T. Radukic, K.M. Müller, Adeno-associated virus capsid protein expression in *Escherichia coli* and chemically defined capsid assembly, *Sci. Rep.* 9 (2019) 18631, doi:10.1038/s41598-019-54928-y.
- [29] Y. Zhang, S. Yin, B. Zhang, J. Bi, Y. Liu, Z. Su, HBC-based virus-like particle assembly from inclusion bodies using 2-methyl-2, 4-pentanediol, *Process Biochem.* 89 (2020) 233–237, doi:10.1016/j.procbio.2019.10.031.
- [30] D.J. Pattinson, S.H. Apte, N. Wibowo, Y.P. Chuan, T. Rivera-Hernandez, P.L. Groves, L.H. Lua, A.P.J. Middelberg, D.L. Doolan, Chimeric murine polyomavirus virus-like particles induce plasmidium antigen-specific CD8<sup>+</sup> T cell and antibody responses, *Front. Cell. Infect. Microbiol.* 9 (2019) 215, doi:10.3389/fcimb.2019.00215.
- [31] M.W.O. Liew, A. Rajendran, A.P.J. Middelberg, Microbial production of virus-like particle vaccine protein at gram-per-litre levels, *J. Biotechnol.* 150 (2010) 224–231, doi:10.1016/j.jbiotec.2010.08.010.
- [32] J. Waneesorn, N. Wibowo, J. Bingham, A.P.J. Middelberg, L.H.L. Lua, Structural-based designed modular capsomere comprising HA1 for low-cost poultry influenza vaccination, *Vaccine* 36 (2016) 3064–3071, doi:10.1016/j.vaccine.2016.11.058.
- [33] N. Wibowo, F.K. Hughes, E.J. Fairmaid, L.H.L. Lua, L.E. Brown, A.P.J. Middelberg, Protective efficacy of a bacterially produced modular capsomere presenting M2e from influenza: extending the potential of broadly cross-protecting epitopes, *Vaccine* 32 (2014) 3651–3655, doi:10.1016/j.vaccine.2014.04.062.
- [34] N. Roos, B. Breiner, L. Preuss, H. Lilie, K. Hipp, H. Herrmann, T. Horn, R. Biener, T. Iftner, C. Simon, Optimized production strategy of the major capsid protein HPV 16L1 non-assembly variant in *E. coli*, *Protein Expr. Purif.* 175 (2020) 105690, doi:10.1016/j.pep.2020.105690.
- [35] N. Hillebrandt, P. Vormittag, N. Bluthardt, A. Dietrich, J. Hubbuch, Integrated process for capture and purification of virus-like particles: enhancing process performance by cross-flow filtration, *Front. Bioeng. Biotechnol.* 8 (2020) 489, doi:10.3389/fbioe.2020.00489.
- [36] J.C. Cook, J.G. Joyce, H.A. George, L.D. Schultz, W.M. Hurni, K.U. Jansen, R.W. Hepler, C. Ip, R.S. Lowe, P.M. Keller, E.D. Lehman, Purification of virus-like particles of recombinant human papillomavirus type 11 major capsid protein L1 from *Saccharomyces cerevisiae*, *Protein Expr. Purif.* 17 (1999) 477–484, doi:10.1006/prep.1999.1155.
- [37] D.I. Lipin, L.H.L. Lua, A.P.J. Middelberg, Quaternary size distribution of soluble aggregates of glutathione-S-transferase-purified viral protein as determined by asymmetrical flow field flow fractionation and dynamic light scattering, *J. Chromatogr. A* 1190 (2008) 204–214, doi:10.1016/j.chroma.2008.03.032.
- [38] N.K. Connors, Y. Wu, L.H.L. Lua, A.P.J. Middelberg, Improved fusion tag cleavage strategies in the downstream processing of self-assembled virus-like particle vaccines, *Food Bioprod. Process.* 92 (2014) 143–151, doi:10.1016/j.fbp.2013.08.012.
- [39] A. Tekewe, N.K. Connors, F. Sainsbury, N. Wibowo, L.H.L. Lua, A.P.J. Middelberg, A rapid and simple screening method to identify conditions for enhanced stability of modular vaccine candidates, *Biochem. Eng. J.* 100 (2015) 50–58, doi:10.1016/j.bej.2015.04.004.
- [40] J. Hirsch, B.W. Faber, J.E. Crowe, B. Verstrepen, G. Cornelissen, *E. coli* production process yields stable dengue 1 virus-sized particles (VSPs), *Vaccine* 38 (2020) 3305–3312, doi:10.1016/j.vaccine.2020.03.003.
- [41] C. Ladd Effio, P. Baumann, C. Weigel, P. Vormittag, A. Middelberg, J. Hubbuch, High-throughput process development of an alternative platform for the production of virus-like particles in *Escherichia coli*, *J. Biotechnol.* 219 (2016) 7–19, doi:10.1016/j.jbiotec.2015.12.018.
- [42] A. Tekewe, Virus-like particle and capsomere vaccines against rotavirus, 2016.
- [43] W.K. Chung, A.S. Freed, M.A. Holstein, S.A. McCallum, S.M. Cramer, Evaluation of protein adsorption and preferred binding regions in multimodal chromatography using NMR, *Proc. Natl. Acad. Sci. U. S. A.* 107 (2010) 16811–16816, doi:10.1073/pnas.1002347107.
- [44] M.M. Bradford, A rapid and sensitive method for the quantitation of microgram quantities of protein utilizing the principle of protein-dye binding, *Anal. Biochem.* 72 (1976) 248–254, doi:10.1016/0003-2697(76)90527-3.
- [45] C. Ladd Effio, L. Wenger, O. Ötes, S.A. Oelmeier, R. Kneusel, J. Hubbuch, Downstream processing of virus-like particles: single-stage and multi-stage aqueous two-phase extraction, *J. Chromatogr. A* 1383 (2015) 35–46, doi:10.1016/j.chroma.2015.01.007.
- [46] M.W.O. Liew, Y.P. Chuan, A.P.J. Middelberg, High-yield and scalable cell-free assembly of virus-like particles by dilution, *Biochem. Eng. J.* 67 (2012) 88–96, doi:10.1016/j.bej.2012.05.007.
- [47] Y. Yuan, E. Shane, C.N. Oliver, Reversed-phase high-performance liquid chromatography of virus-like particles, *J. Chromatogr. A* 816 (1998) 21–28, doi:10.1016/S0021-9673(98)00065-X.
- [48] B.K. Nfor, M. Noverraz, S. Chilamkurthi, P.D.E.M. Verhaert, L.A.M. van der Wiele, M. Ottens, High-throughput isotherm determination and thermodynamic modeling of protein adsorption on mixed mode adsorbents, *J. Chromatogr. A* 1217 (2010) 6829–6850, doi:10.1016/j.chroma.2010.07.069.

- [49] Cytiva, Uppsala, Sweden, Instructions 11003505 AF - Capto™ MMC, 2018. <https://cdn.cytivalifesciences.com/dmm3bwsv3/AssetStream.aspx?mediaformatid=10061&destinationid=10016&assetid=13701> (accessed 25 January 2021).
- [50] D. Chang, X. Cai, R.A. Consigli, Characterization of the DNA binding properties of polyomavirus capsid protein, *J. Virol.* 67 (1993) 6327–6331, doi:10.1128/jvi.67.10.6327-6331.1993.
- [51] C. Tarmann, A. Jungbauer, Adsorption of plasmid DNA on anion exchange chromatography media, *J. Sep. Sci.* 31 (2008) 2605–2618, doi:10.1002/jssc.200700654.
- [52] M. Friedman, M.R. Gumbmann, P.M. Masters, Protein-alkali reactions: chemistry, toxicology, and nutritional consequences, *Adv. Exp. Med. Biol.* 177 (1984) 367–412, doi:10.1007/978-1-4684-4790-3\_18.
- [53] G. Zhao, X.-Y. Dong, Y. Sun, Ligands for mixed-mode protein chromatography: principles, characteristics and design, *J. Biotechnol.* 144 (2009) 3–11, doi:10.1016/j.jbiotec.2009.04.009.
- [54] Cytiva, Uppsala, Sweden, Data File 11-0035-45 AA, 2005. <https://www.cytivalifesciences.co.jp/newsletter/downstream/pdf/11003545aa.pdf> (accessed 25 January 2021)
- [55] C. Ladd Effio, T. Hahn, J. Seiler, S.A. Oelmeier, I. Asen, C. Silberer, L. Villain, J. Hubbuch, Modeling and simulation of anion-exchange membrane chromatography for purification of Sf9 insect cell-derived virus-like particles, *J. Chromatogr. A* 1429 (2016) 142–154, doi:10.1016/j.chroma.2015.12.006.
- [56] D.I. Lipin, A. Raj, L.H.L. Lua, A.P.J. Middelberg, Affinity purification of viral protein having heterogeneous quaternary structure: modeling the impact of soluble aggregates on chromatographic performance, *J. Chromatogr. A* 1216 (2009) 5696–5708, doi:10.1016/j.chroma.2009.05.082.
- [57] N. Hammerschmidt, S. Hobiger, A. Jungbauer, Continuous polyethylene glycol precipitation of recombinant antibodies: sequential precipitation and resolubilization, *Process Biochem.* 51 (2016) 325–332, doi:10.1016/j.procbio.2015.11.032.
- [58] Y. Ding, Y.P. Chuan, L. He, A.P.J. Middelberg, Modeling the competition between aggregation and self-assembly during virus-like particle processing, *Biotechnol. Bioeng.* 107 (2010) 550–560, doi:10.1002/bit.22821.
- [59] X.S. Chen, G. Casini, S.C. Harrison, R.L. Garcea, Papillomavirus capsid protein expression in *Escherichia coli*: purification and assembly of HPV11 and HPV16 L1, *J. Mol. Biol.* 307 (2001) 173–182, doi:10.1006/jmbi.2000.4464.
- [60] L.R. Chromy, J.M. Pipas, R.L. Garcea, Chaperone-mediated in vitro assembly of polyomavirus capsids, *Proc. Natl. Acad. Sci. U. S. A.* 100 (2003) 10477–10482, doi:10.1073/pnas.1832245100.
- [61] O. Genest, S. Wickner, S.M. Doyle, Hsp90 and Hsp70 chaperones: collaborators in protein remodeling, *J. Biol. Chem.* 294 (2019) 2109–2120, doi:10.1074/jbc.REV118.002806.
- [62] R. Westermeier, Frequently made mistakes in electrophoresis, *Proteomics* 7 (Suppl 1) (2007) 60–63, doi:10.1002/pmic.200790077.
- [63] J.H. Bowen, V. Chlumecky, P. D'Obrenan, J.S. Colter, Evidence that polyoma polypeptide VP1 is a serine protease, *Virology* 135 (1984) 551–554, doi:10.1016/0042-6822(84)90210-1.